

## Supporting Information

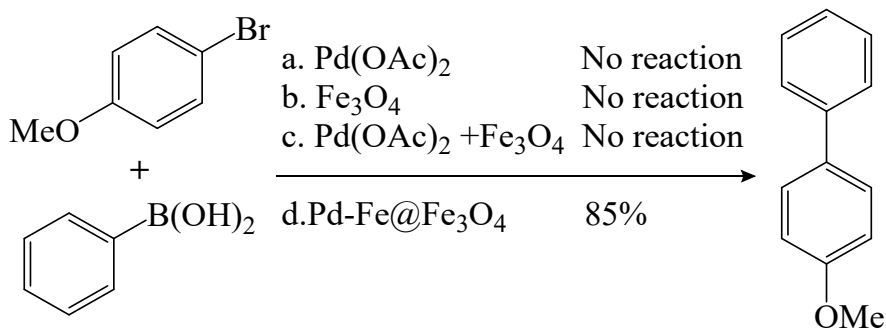
### Magnetic Pd-Fe Nanoparticles for Sustainable Suzuki-Miyaura Cross-coupling Reactions

#### List of Contents

1. Controlled Catalytic Reaction and Calculation of Pd% loading-----	S1
2. XPS details of Fe-Pd@Fe <sub>3</sub> O <sub>4</sub> -----	S2
3. EDAX mapping details of Fe-Pd@Fe <sub>3</sub> O <sub>4</sub> -----	S3
4. SEM images of Fe-Pd@Fe <sub>3</sub> O <sub>4</sub> -----	S4
5. FT-IR analysis of Fe-Pd@Fe <sub>3</sub> O <sub>4</sub> -----	S5
6. Characterization of the Products-----	S6-S8
7. Copies of <sup>1</sup> H-NMR and <sup>13</sup> C-NMR Spectra-----	S9-S19

## 1. Controlled Catalytic Reactions and Calculation of Pd% loading

It was found that successful couplings require the presence of Pd-Fe@Fe<sub>3</sub>O<sub>4</sub>, as determined by the control reactions in preliminary experiment in Scheme S1, where only reaction catalyzed by prepared Pd-Fe@Fe<sub>3</sub>O<sub>4</sub> containing 320ppm gave 85% yield while reactions that we attempted using equal amounts of Pd(OAc)<sub>2</sub>, Fe<sub>3</sub>O<sub>4</sub>, or Pd(OAc)<sub>2</sub> and Fe<sub>3</sub>O<sub>4</sub> did not lead to product formation.

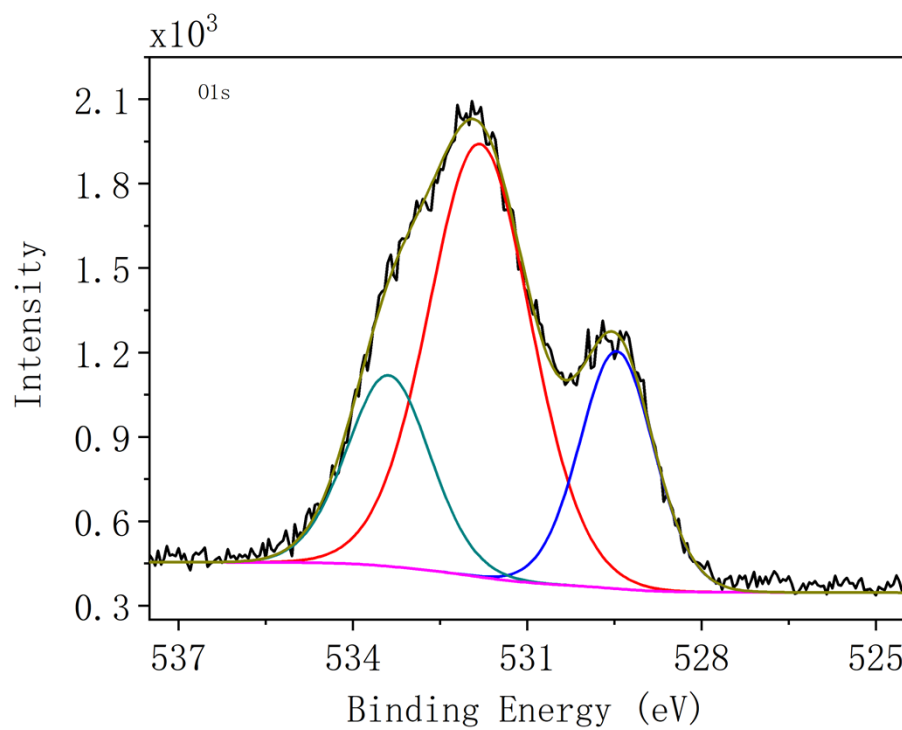
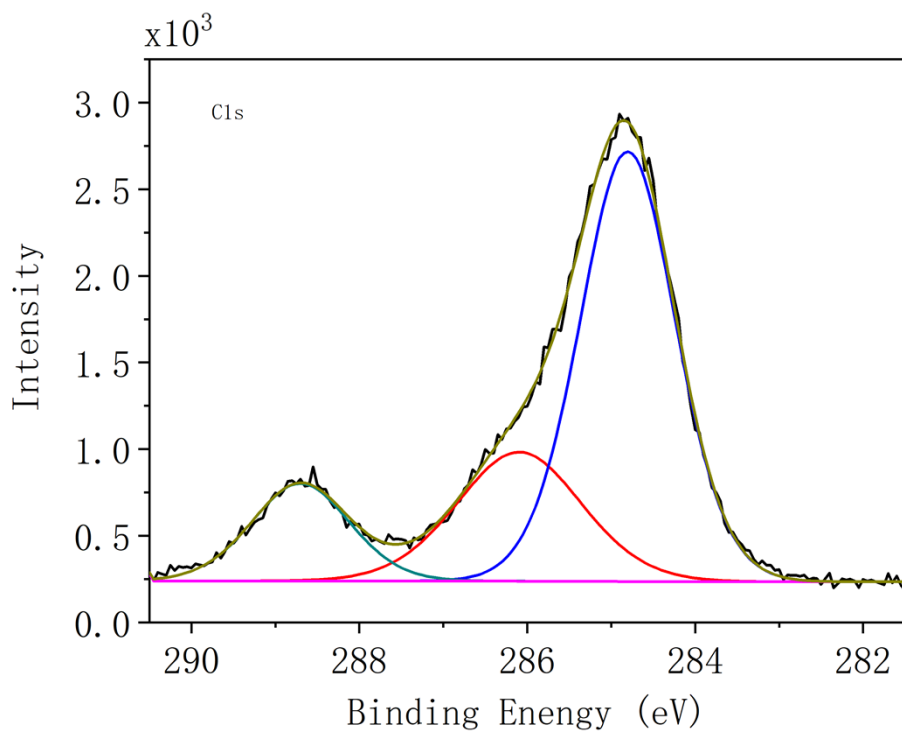


Scheme S1 Control reactions proved the importance of Pd-Fe@Fe<sub>3</sub>O<sub>4</sub>

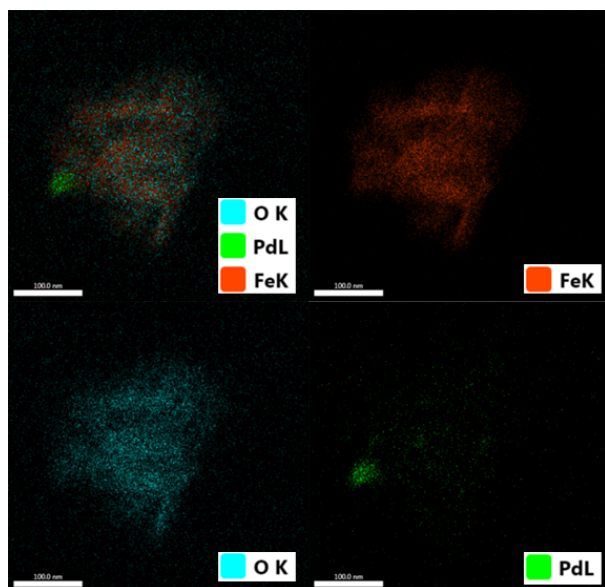
The Pd loading was determined based on the actual amount of Pd utilized in the preparation of the catalyst, rather than the nominal loading with the following formula:

$$\begin{aligned} \text{Pd mol\%} &= \frac{n(\text{Pd(OAc)}_2) * \frac{m(\text{catalyst in a reaction})}{m_0(\text{all prepared catalyst})}}{n(\text{reaction})} * 100\% \\ &= \frac{0.027\text{mmol} * \frac{0.825\text{mg}}{110\text{mg}}}{0.5\text{mmol}} * 100\% \end{aligned}$$

## 2. XPS details of Fe-Pd@Fe<sub>3</sub>O<sub>4</sub>

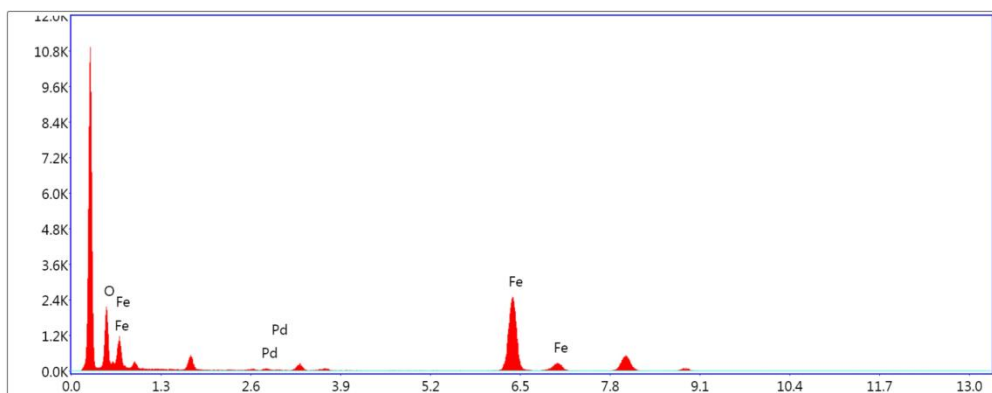


### 3. EDAX mapping details of Fe-Pd@Fe<sub>3</sub>O<sub>4</sub>



kV: 200 Mag:160000 Takeoff:14.8 Live Time(s):38.9 Amp Time(μs):7.68 Resolution(eV):127.6

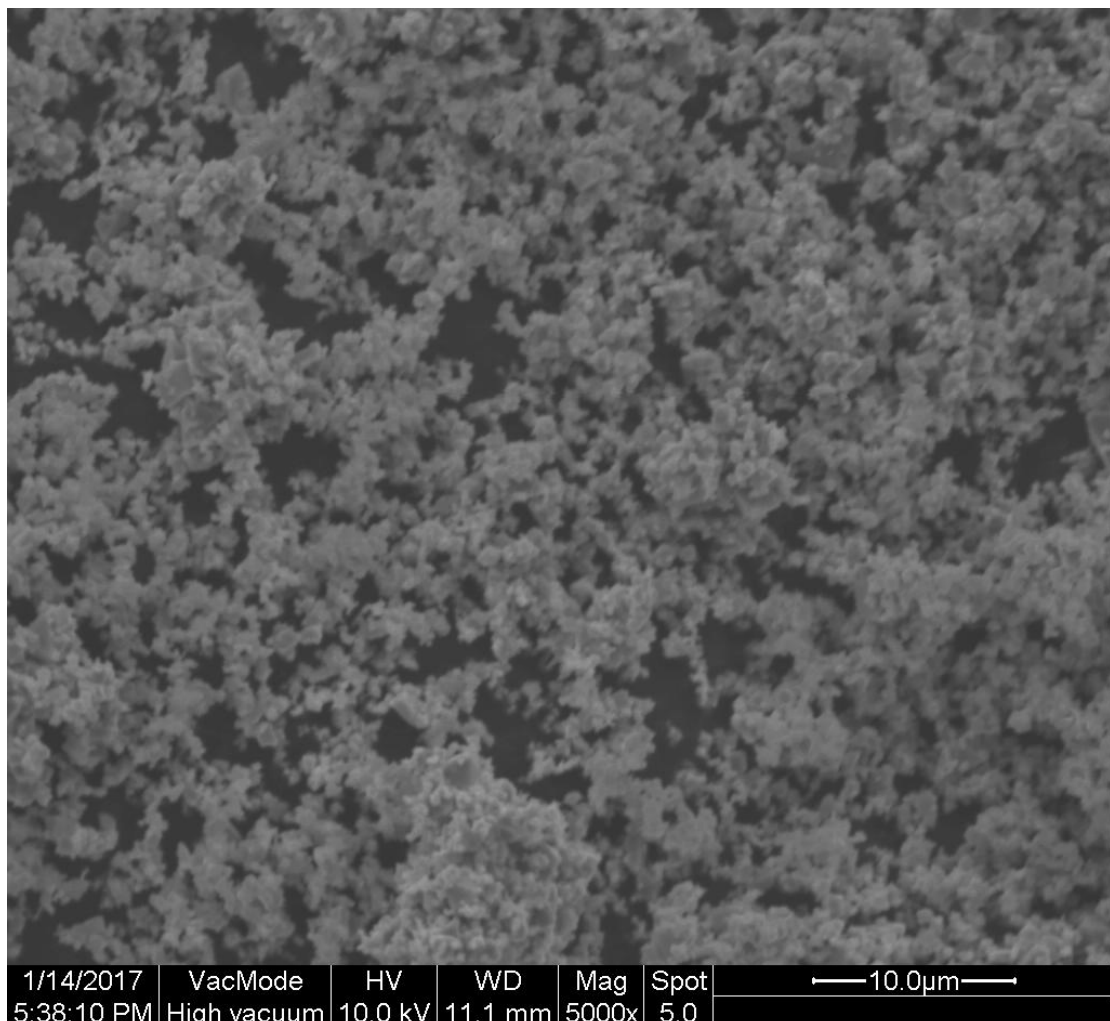
**Phase: O K/FeK**



**MThin Smart Quant Results (Theoretical)**

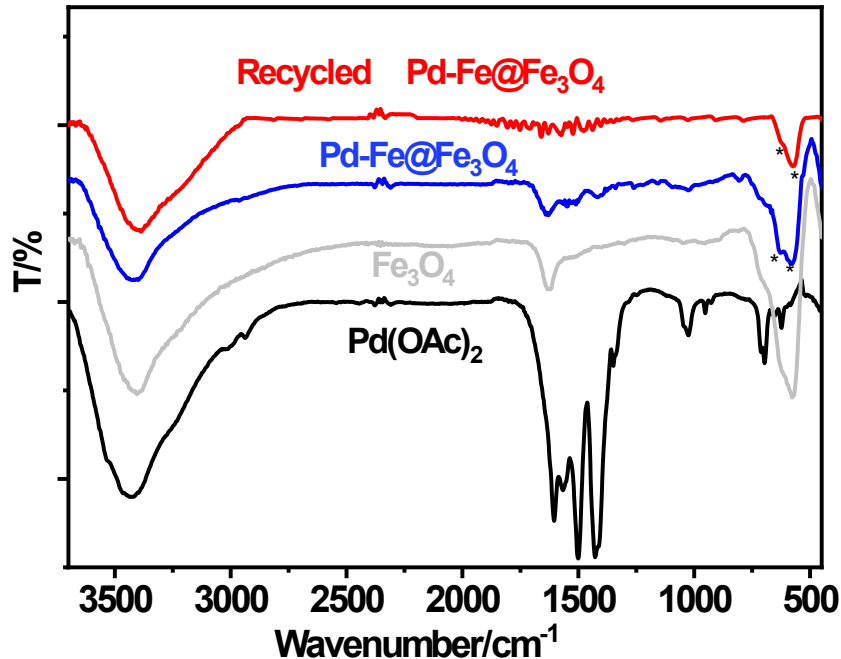
Element	Weight %	Atomic %	Net Int.	Net	KABFacto
O K	22.78	51.30	346.7	0.96	0.8
PdL	3.62	1.23	16.7	5.74	2.65
FeK	73.60	47.47	898.5	0.62	1

#### 4. SEM images of Fe-Pd@Fe<sub>3</sub>O<sub>4</sub>



1/14/2017	VacMode	HV	WD	Mag	Spot	10.0μm
5:38:10 PM	High vacuum	10.0 kV	11.1 mm	5000x	5.0	

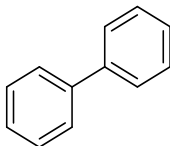
## 5. FT-IR analysis of Fe-Pd@Fe<sub>3</sub>O<sub>4</sub>



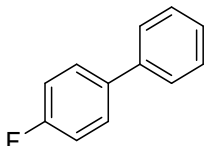
FT-IR of recycled Pd-Fe@Fe<sub>3</sub>O<sub>4</sub>, Pd-Fe@Fe<sub>3</sub>O<sub>4</sub>, Fe<sub>3</sub>O<sub>4</sub> and Pd(OAc)<sub>2</sub>

Fourier transform infrared (FT-IR) spectroscopy analysis of the recycled Pd-Fe@Fe<sub>3</sub>O<sub>4</sub>, Pd-Fe@Fe<sub>3</sub>O<sub>4</sub>, Fe<sub>3</sub>O<sub>4</sub> and Pd(OAc)<sub>2</sub> was displayed. As we all know, the peaks around 3400 and 1600 wavenumbers are hydroxyl absorption peaks and the peaks around 2350 wavenumbers are O=C=O absorption peaks in the environment, while the infrared characteristic peaks of Fe-O bonds are generally below 700 wavenumbers. Comparing the infrared absorption curves of Pd-Fe@Fe<sub>3</sub>O<sub>4</sub> and Fe<sub>3</sub>O<sub>4</sub>, we find that the absorption peak is divided from 577 wavenumber splitting into 628 and 578 wavenumbers, respectively, which is likely caused by the introduction of additional iron. At the same time, comparing the infrared absorption curve of Pd(OAc)<sub>2</sub>, we found that the characteristic peak of acetate disappeared, indicating that palladium was completely reduced. The infrared absorption curve of recycled Pd-Fe@Fe<sub>3</sub>O<sub>4</sub> showed that the nano-catalyst remain a stable structure after a gram-scale reaction.

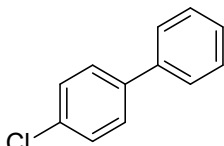
## 6. Characterization of the Products.



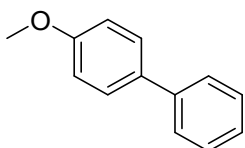
**1,1'-biphenyl.**  $^1\text{H}$  NMR (400 MHz,  $\text{CDCl}_3$ )  $\delta$  (ppm): 7.51 (d,  $J = 7.6$  Hz, 4H), 7.35 (t,  $J = 7.5$  Hz, 4H), 7.25 (t,  $J = 7.3$  Hz, 2H).  $^{13}\text{C}$  NMR (101 MHz,  $\text{CDCl}_3$ )  $\delta$  (ppm): 141.37, 128.88, 127.38, 127.30.



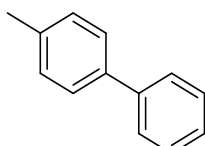
**4-fluoro-1,1'-biphenyl.**  $^1\text{H}$  NMR (400 MHz,  $\text{CDCl}_3$ )  $\delta$  (ppm): 7.42 (d,  $J = 7.9$  Hz, 4H), 7.31 (t,  $J = 7.4$  Hz, 2H), 7.22 (t,  $J = 7.2$  Hz, 1H), 7.00 (t,  $J = 8.2$  Hz, 2H).  $^{13}\text{C}$  NMR (101 MHz,  $\text{CDCl}_3$ )  $\delta$  (ppm): 162.4 (d,  $J = 246.3$ ), 140.2, 137.3 (d,  $J = 3.3$ ), 128.8, 128.6 (d,  $J = 8.0$ ).



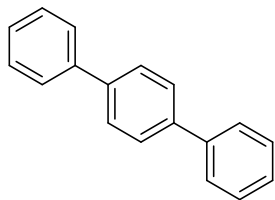
**4-chloro-1,1'-biphenyl.**  $^1\text{H}$  NMR (400 MHz,  $\text{CDCl}_3$ )  $\delta$  (ppm): 7.40 (dd,  $J = 16.5$ , 8.0 Hz, 4H), 7.28 (dt,  $J = 20.7$ , 9.9 Hz, 5H).  $^{13}\text{C}$  NMR (101 MHz,  $\text{CDCl}_3$ )  $\delta$  (ppm): 138.57, 127.83, 127.80, 127.30, 126.51, 125.89.



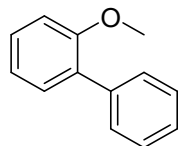
**4-methoxy-1,1'-biphenyl.**  $^1\text{H}$  NMR (400 MHz,  $\text{CDCl}_3$ )  $\delta$  (ppm): 7.42 (t,  $J = 9.1$  Hz, 4H), 7.29 (t,  $J = 7.5$  Hz, 2H), 7.18 (t,  $J = 7.3$  Hz, 1H), 6.85 (d,  $J = 8.3$  Hz, 2H), 3.70 (s, 3H).  $^{13}\text{C}$  NMR (101 MHz,  $\text{CDCl}_3$ )  $\delta$  (ppm): 159.25, 140.90, 133.85, 128.81, 128.22, 126.81, 126.74, 114.31, 55.38.



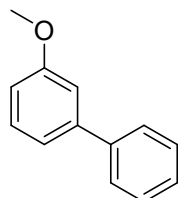
**4-methyl-1,1'-biphenyl.**  $^1\text{H}$  NMR (400 MHz,  $\text{CDCl}_3$ )  $\delta$  (ppm): 7.44 (d,  $J = 7.5$  Hz, 2H), 7.36 (d,  $J = 7.6$  Hz, 2H), 7.28 (t,  $J = 7.3$  Hz, 2H), 7.18 (t,  $J = 7.3$  Hz, 1H), 7.10 (d,  $J = 7.7$  Hz, 2H), 2.25 (s, 3H).  $^{13}\text{C}$  NMR (101 MHz,  $\text{CDCl}_3$ )  $\delta$  (ppm): 141.25, 138.45, 137.07, 129.57, 128.84, 128.80, 127.08, 127.05, 21.17.



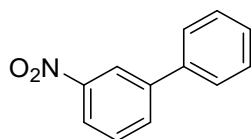
**1,1',4',1''-terphenyl.**  $^1\text{H}$  NMR (400 MHz,  $\text{CDCl}_3$ )  $\delta$  (ppm): 7.63 – 7.54 (m), 7.38 (t,  $J = 7.5$  Hz), 7.28 (t,  $J = 7.3$  Hz).  $^{13}\text{C}$  NMR (101 MHz,  $\text{CDCl}_3$ )  $\delta$  (ppm): 139.67, 139.09, 127.78, 126.46, 126.30, 126.01.



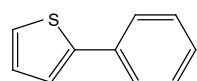
**2-methoxy-1,1'-biphenyl.**  $^1\text{H}$  NMR (400 MHz,  $\text{CDCl}_3$ )  $\delta$  (ppm): 7.42 (d,  $J = 7.9$  Hz, 2H), 7.29 (t,  $J = 7.4$  Hz, 2H), 7.20 (t,  $J = 8.4$  Hz, 3H), 6.91 (t,  $J = 7.4$  Hz, 1H), 6.85 (d,  $J = 8.1$  Hz, 1H), 3.66 (s, 3H).  $^{13}\text{C}$  NMR (101 MHz,  $\text{CDCl}_3$ )  $\delta$  (ppm): 156.57, 138.66, 130.97, 130.84, 129.64, 128.70, 128.06, 126.99, 120.93, 111.36, 55.60.



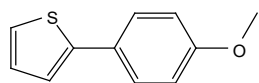
**3-methoxy-1,1'-biphenyl.**  $^1\text{H}$  NMR (400 MHz,  $\text{CDCl}_3$ )  $\delta$  (ppm): 7.48 (d,  $J = 7.6$  Hz, 2H), 7.32 (t,  $J = 7.3$  Hz, 2H), 7.28 – 7.17 (m, 2H), 7.08 (d,  $J = 7.6$  Hz, 1H), 7.03 (s, 1H), 6.79 (d,  $J = 8.1$  Hz, 1H), 3.74 (s, 3H).  $^{13}\text{C}$  NMR (101 MHz,  $\text{CDCl}_3$ )  $\delta$  (ppm): 158.89, 141.71, 140.04, 128.69, 127.67, 126.35, 126.13, 118.62, 111.85, 111.62, 54.21.



**3-nitro-1,1'-biphenyl.**  $^1\text{H}$  NMR (400 MHz,  $\text{CDCl}_3$ )  $\delta$  (ppm): 8.30 (s, 1H), 8.05 (d,  $J = 8.0$  Hz, 1H), 7.77 (d,  $J = 7.7$  Hz, 1H), 7.53 – 7.44 (m, 3H), 7.33 (dt,  $J = 24.6, 7.2$  Hz, 3H).  $^{13}\text{C}$  NMR (101 MHz,  $\text{CDCl}_3$ )  $\delta$  (ppm): 148.73, 142.84, 138.63, 133.03, 129.73, 129.18, 128.56, 127.15, 122.02, 121.90.

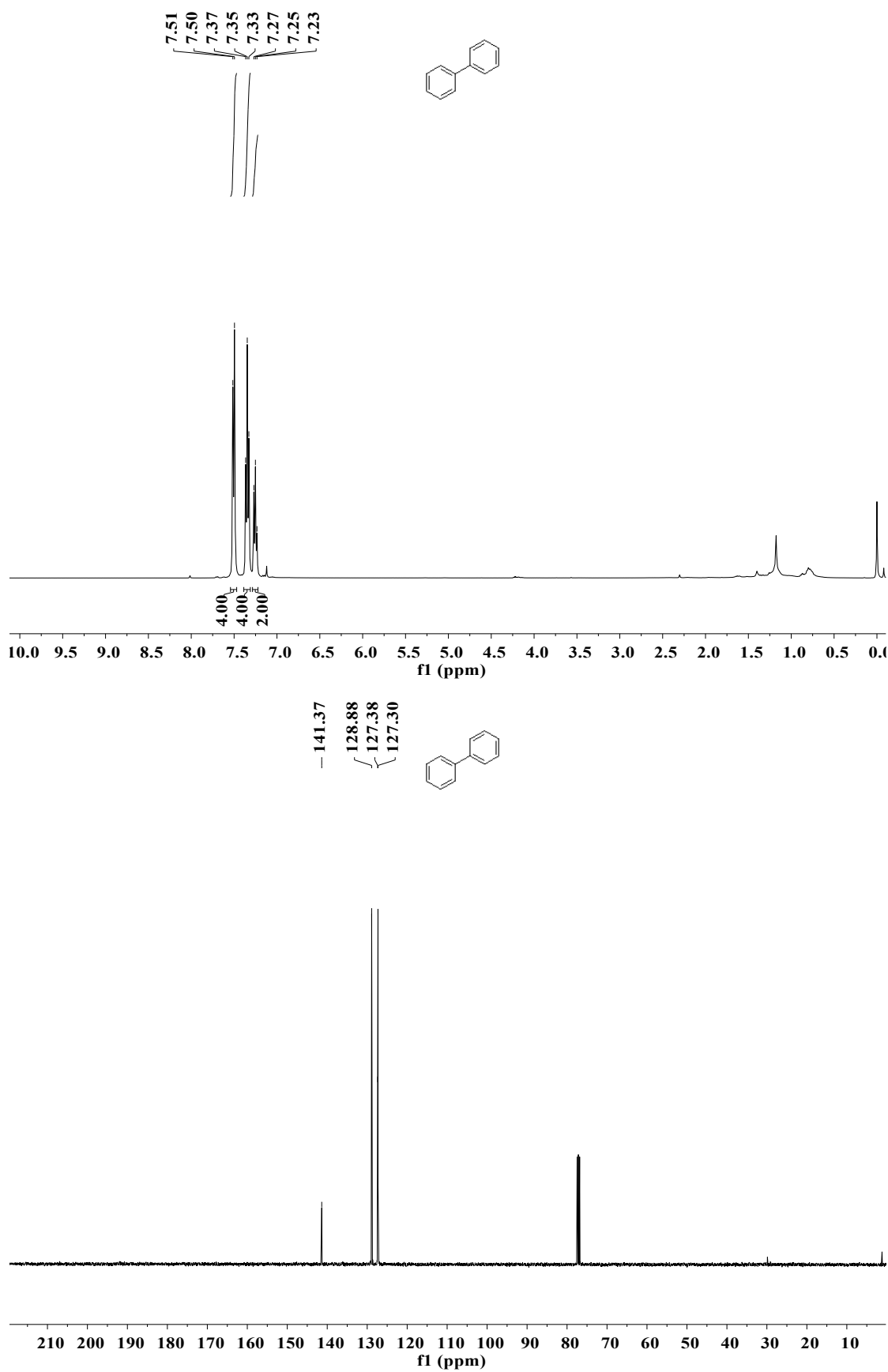


**2-Phenylthiophene.** <sup>1</sup>H NMR (400 MHz, CDCl<sub>3</sub>) δ (ppm): 7.66 – 7.60 (m, 2H), 7.39 (t, J = 7.6 Hz, 2H), 7.35 – 7.31 (m, 1H), 7.29 (dd, J = 5.7, 3.8 Hz, 2H), 7.09 (dd, J = 5.0, 3.7 Hz, 1H). <sup>13</sup>C NMR (101 MHz, CDCl<sub>3</sub>) δ (ppm): 144.51, 134.47, 128.97, 128.10, 127.55, 126.04, 124.90, 123.16.

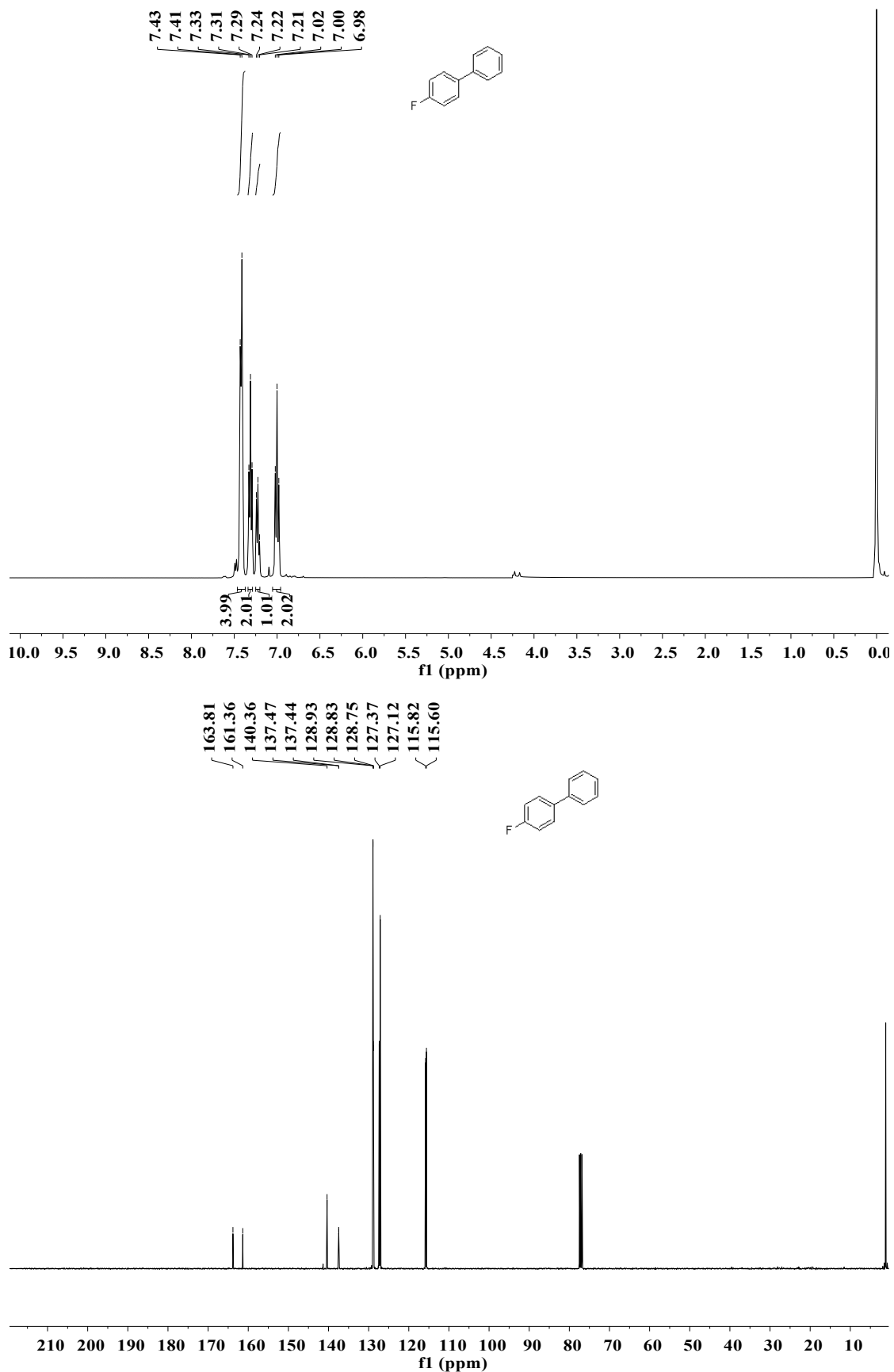


**1-(4-Thiophen-2-yl-phenyl)-ethanon.** <sup>1</sup>H NMR (400 MHz, CDCl<sub>3</sub>) δ (ppm): 7.54 (d, J = 8.7 Hz, 2H), 7.21 (d, J = 5.8 Hz, 1H), 7.20 (d, 1H), 7.05 (dd, J = 4.9, 3.7 Hz, 1H), 6.92 (d, J = 8.8 Hz, 2H), 3.84 (s, 3H). <sup>13</sup>C NMR (101 MHz, CDCl<sub>3</sub>) δ (ppm): 159.23, 144.40, 128.01, 127.36, 127.30, 123.92, 122.16, 114.33, 55.45.

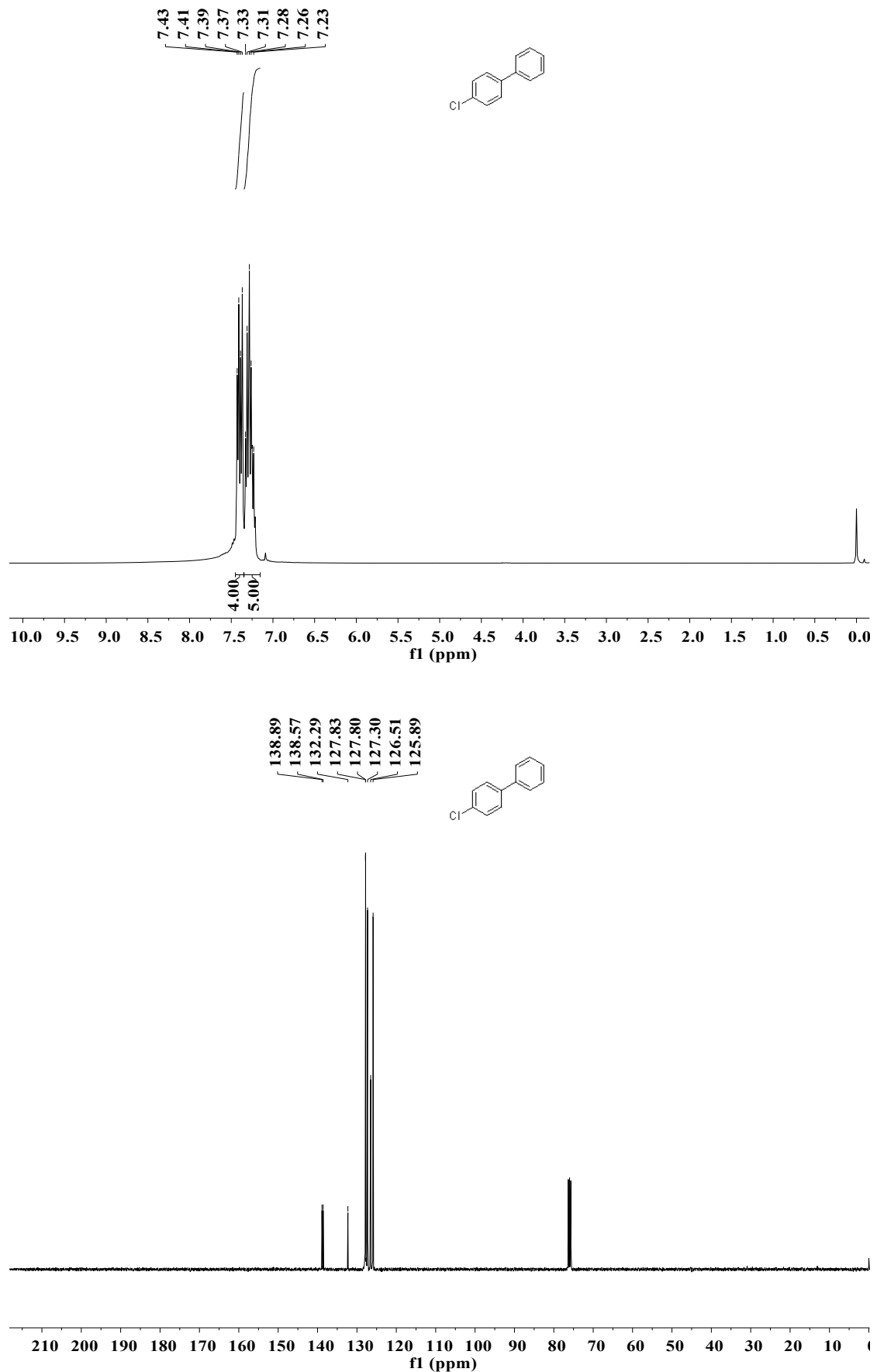
**7. Copies of  $^1\text{H}$ -NMR and  $^{13}\text{C}\{^1\text{H}\}$  NMR Spectra.**



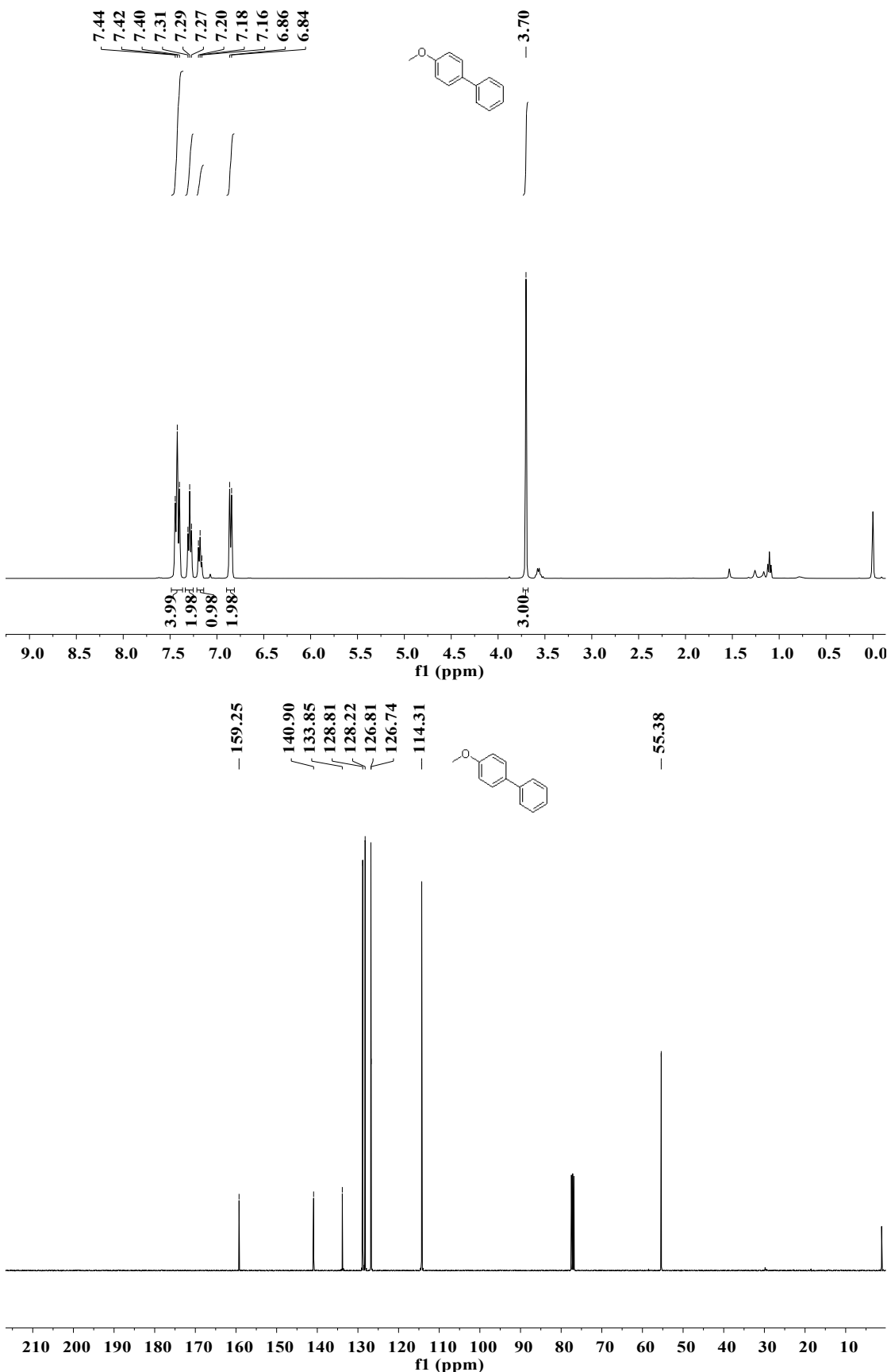
$^1\text{H}$  NMR (400 MHz) and  $^{13}\text{C}\{^1\text{H}\}$  NMR (101 MHz) spectra of 1,1'-biphenyl ( $\text{CDCl}_3$ ).

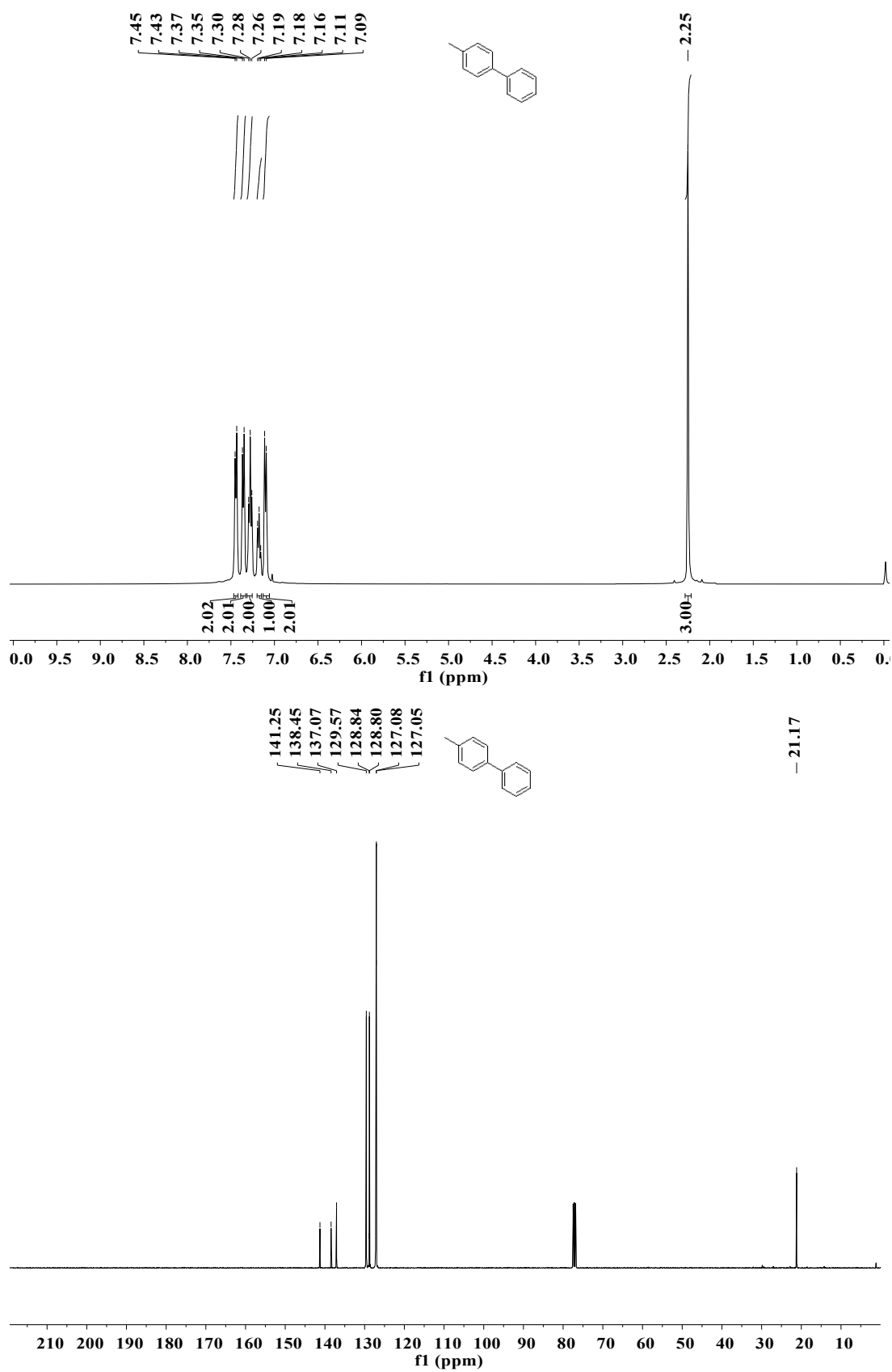


$^1\text{H}$  NMR (400 MHz) and  $^{13}\text{C}\{^1\text{H}\}$  NMR (101 MHz) spectra of 4-fluoro-1,1'-biphenyl ( $\text{CDCl}_3$ ).

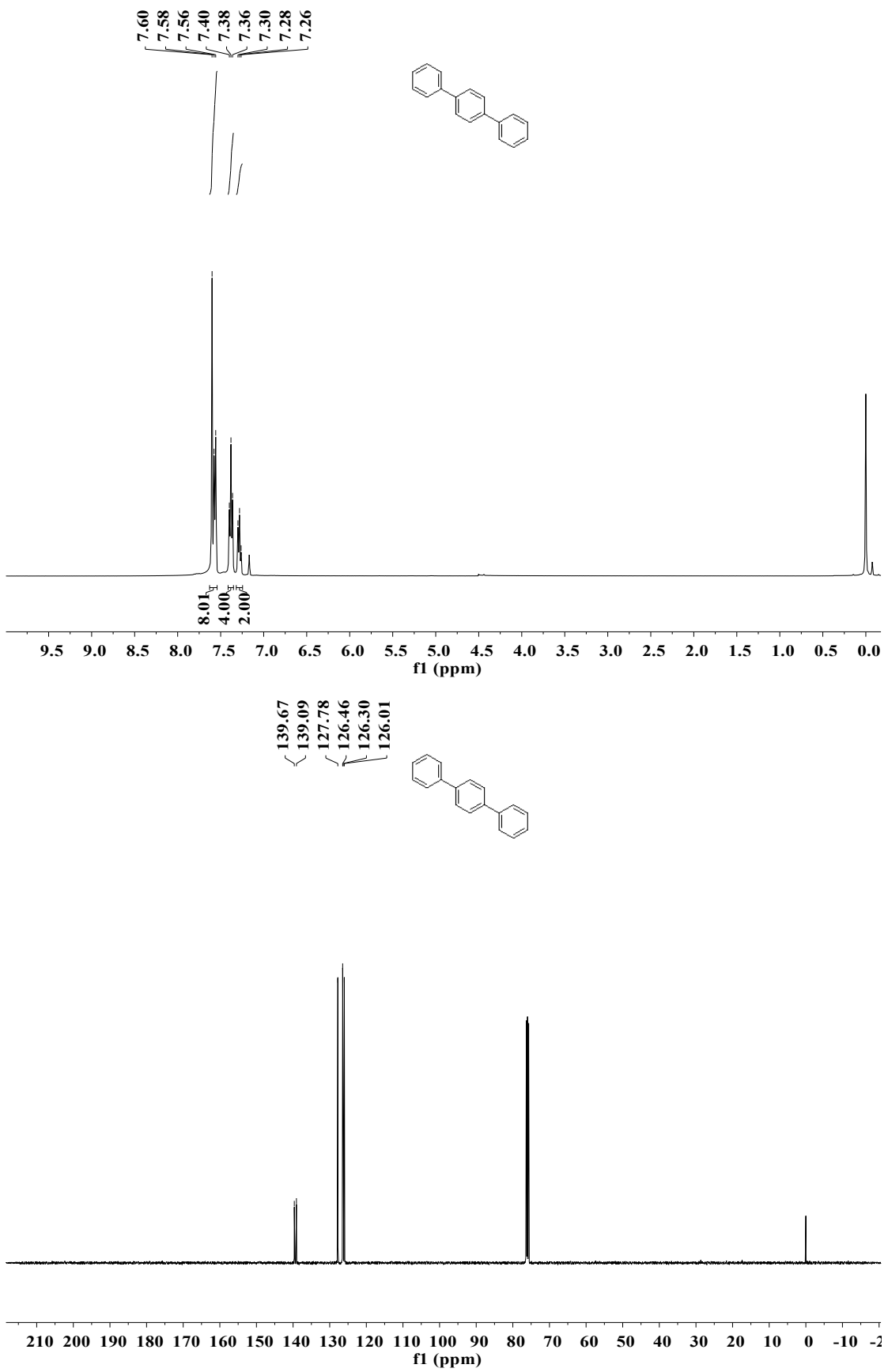


$^1\text{H}$  NMR (400 MHz) and  $^{13}\text{C}\{^1\text{H}\}$  NMR (101 MHz) spectra of 4-chloro-1,1'-biphenyl ( $\text{CDCl}_3$ ).

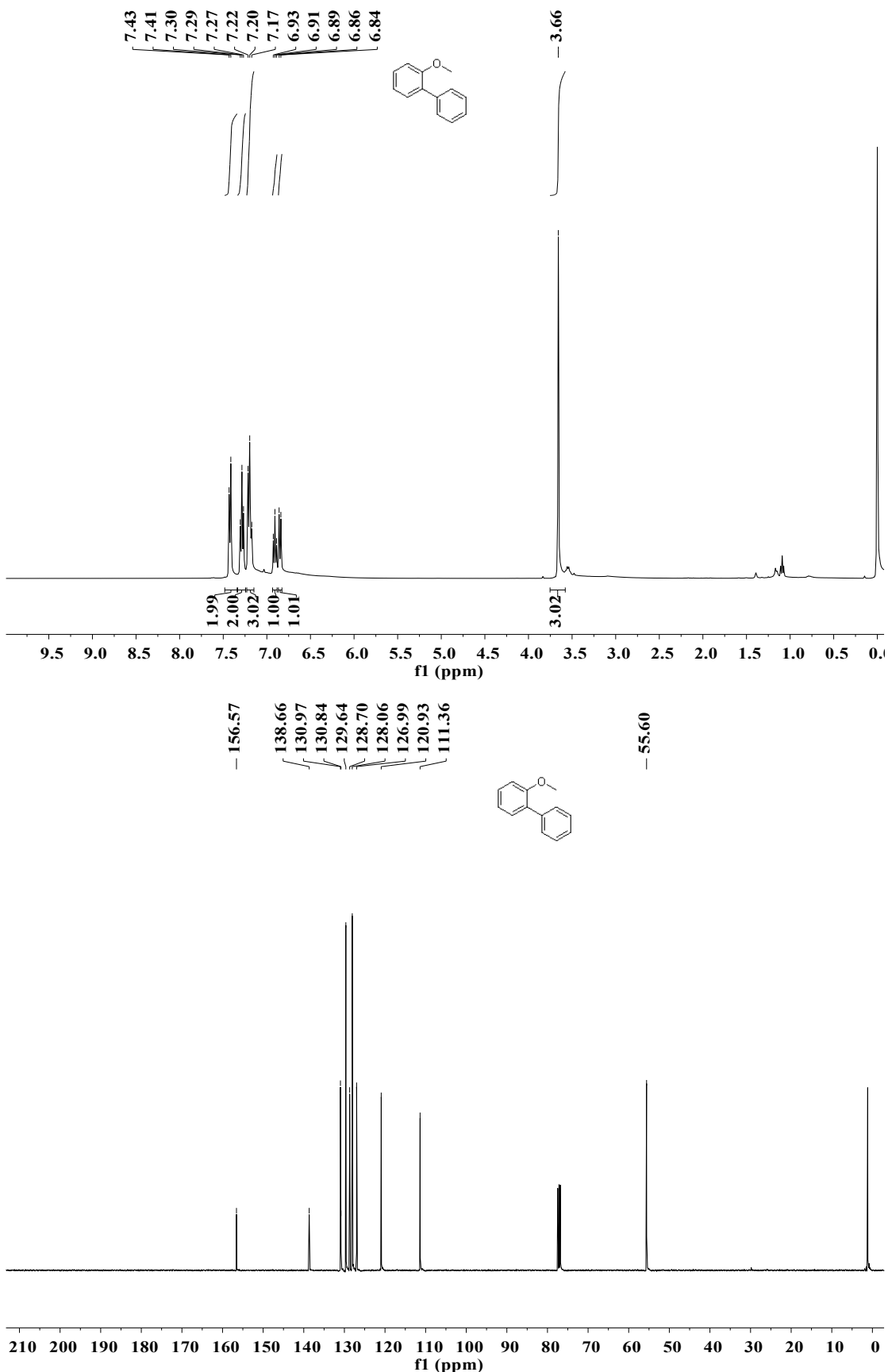


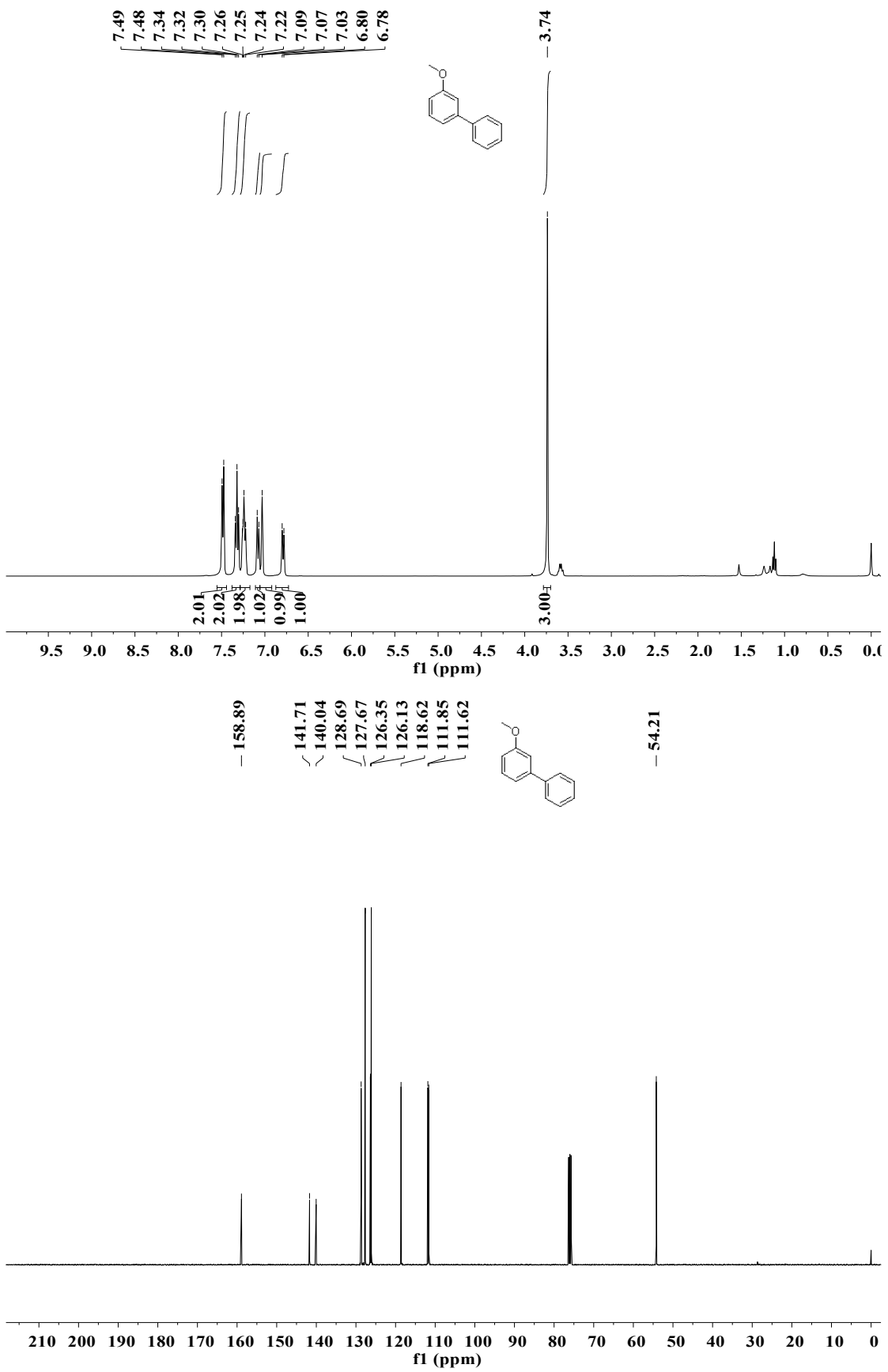


$^1\text{H}$  NMR (400 MHz) and  $^{13}\text{C}\{^1\text{H}\}$  NMR (101 MHz) spectra of 4-methyl-1,1'-biphenyl ( $\text{CDCl}_3$ ).

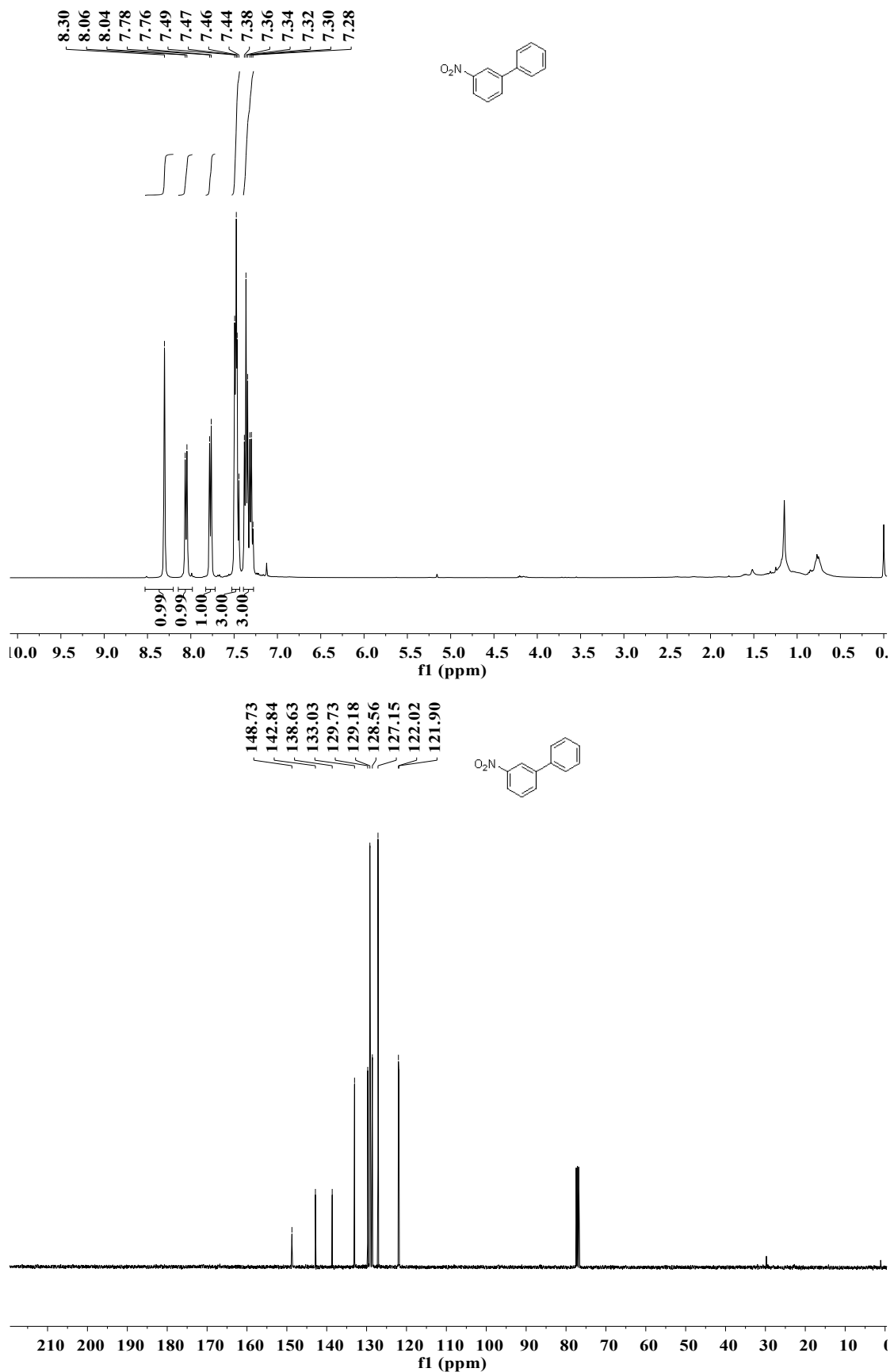


$^1\text{H}$  NMR (400 MHz) and  $^{13}\text{C}\{\text{H}\}$  NMR (101 MHz) spectra of 1,1',4',1''-terphenyl ( $\text{CDCl}_3$ ).

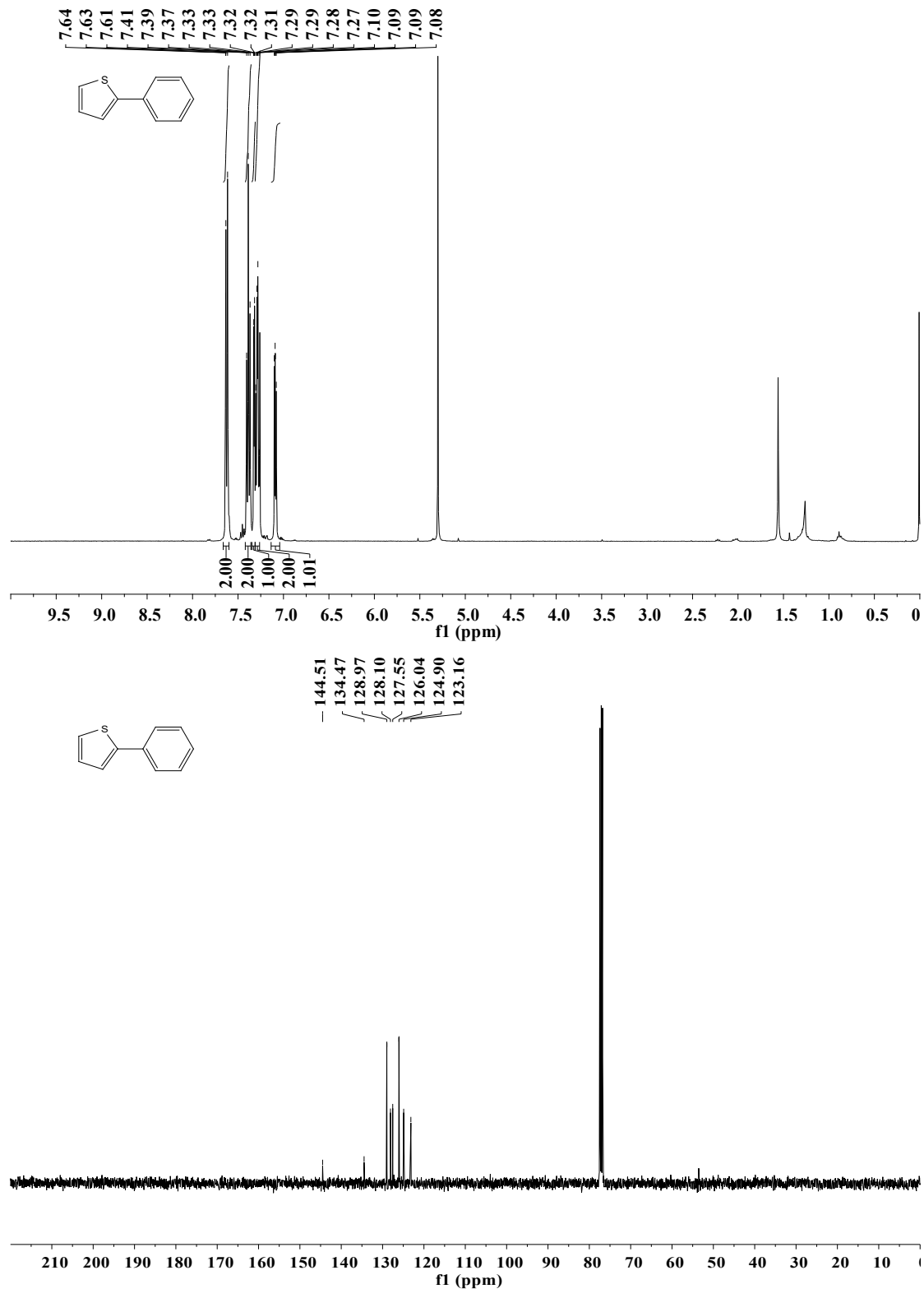


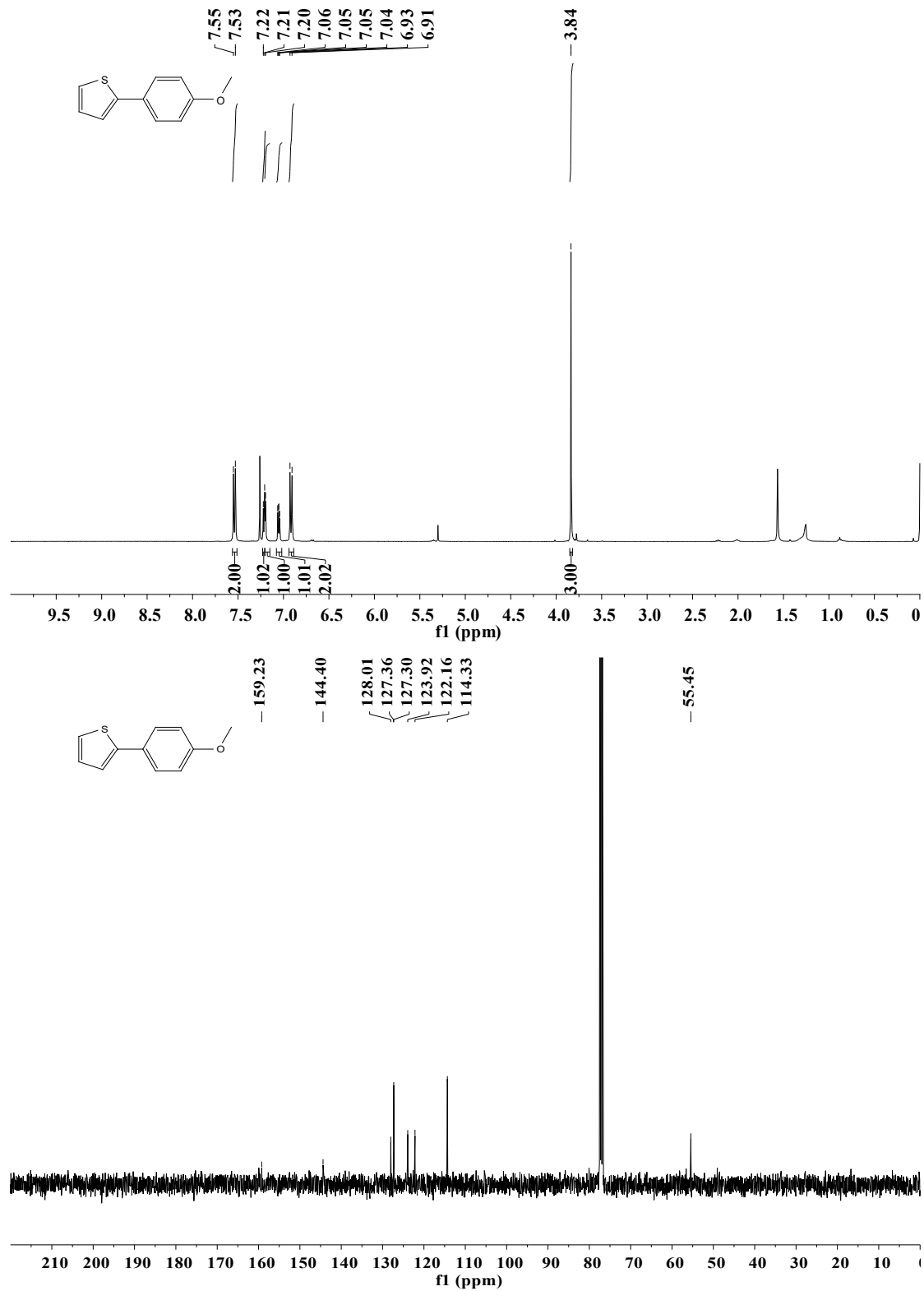


$^1\text{H}$  NMR (400 MHz) and  $^{13}\text{C}\{^1\text{H}\}$  NMR (101 MHz) spectra of 3-methoxy-1,1'-biphenyl ( $\text{CDCl}_3$ ).



$^1\text{H}$  NMR (400 MHz) and  $^{13}\text{C}\{^1\text{H}\}$  NMR (101 MHz) spectra of 3-nitro-1,1'-biphenyl ( $\text{CDCl}_3$ ).





<sup>1</sup>H NMR (400 MHz) and <sup>13</sup>C{<sup>1</sup>H} NMR (101 MHz) spectra of 1-(4-Thiophen-2-yl-phenyl)-ethanon ( $\text{CDCl}_3$ ).